Design, Synthesis, Structural and Functional Characterization of Novel Melanocortin Agonists Based on the Cyclotide Kalata B1[*]

Rasmus Eliasen[‡§], **Norelle L. Daly**[¶‖][1], **Birgitte S. Wulff**[‡], **Thomas L. Andresen**[§], **Kilian W. Conde-Frieboes**[‡], and **David J. Craik**[‖][2]

From [‡]Novo Nordisk A/S, 2760 Måløv, Denmark, the [¶]Queensland Tropical Health Alliance, School of Pharmacy and Molecular Sciences and Centre for Biodiscovery and Molecular Development of Therapeutics, James Cook University, Cairns, Queensland 4870, Australia, the [‖]Institute for Molecular Bioscience, University of Queensland, Brisbane, Queensland 4072, Australia, and the [§]Department of Micro- and Nanotechnology, Center for Nanomedicine and Theranostics, Technical University of Denmark, 2800 Kongens Lyngby, Denmark

Background: Cyclotides are useful scaffolds to stabilize bioactive peptides.
Results: Four melanocortin analogues of kalata B1 were synthesized. One is a selective MC4R agonist.
Conclusion: The analogues retain the native kalata B1 scaffold and introduce a designed pharmacological activity, validating cyclotides as protein engineering scaffolds.
Significance: A novel type of melanocortin agonist has been developed, with potential as a drug lead for treating obesity.

Obesity is an increasingly important global health problem that lacks current treatment options. The melanocortin receptor 4 (MC4R) is a target for obesity therapies because its activation triggers appetite suppression and increases energy expenditure. Cyclotides have been suggested as scaffolds for the insertion and stabilization of pharmaceutically active peptides. In this study, we explored the development of appetite-reducing peptides by synthesizing MC4R agonists based on the insertion of the His-Phe-Arg-Trp sequence into the cyclotide kalata B1. The ability of the analogues to fold similarly to kalata B1 but display MC4R activity were investigated. Four peptides were synthesized using *t*-butoxycarbonyl peptide chemistry with a C-terminal thioester to facilitate backbone cyclization. The structures of the peptides were found to be similar to kalata B1, evaluated by Hα NMR chemical shifts. KB1(GHFRWG;23–28) had a K_i of 29 nM at the MC4R and was 107 or 314 times more selective over this receptor than MC1R or MC5R, respectively, and had no detectable binding to MC3R. The peptide had higher affinity for the MC4R than the endogenous agonist, α-melanocyte stimulation hormone, but it was less potent at the MC4R, with an EC$_{50}$ of 580 nM for activation of the MC4R. In conclusion, we synthesized melanocortin analogues of kalata B1 that preserve the structural scaffold and display receptor binding and functional activity. KB1(GHFRWG;23–28) is potent and selective for the MC4R. This compound validates the use of cyclotides as scaffolds and has the potential to be a new lead for the treatment of obesity.

Obesity is an increasing problem world wide with 1.5 billion adults estimated to be overweight (body mass index above 25 kg/m^2) and 500 million obese (body mass index above 30 kg/m^2) in 2008 (1). These statistics are alarming given that obesity is associated with a risk of developing a variety of debilitating diseases, including type 2 diabetes, cardiovascular disease, and hypertension (2–4). To prevent or reduce obesity and the risk of related diseases, regular exercise and a healthy diet are very effective (5), but in high risk patients drug treatment is also necessary (6). Currently, only two drugs are approved for the treatment of obesity, *i.e.* orlistat and phentermine. The Food and Drug Administration withdrew sibutramine in 2010 because of increased risk of cardiovascular events (7). Although drugs currently on the market for other indications are undergoing clinical trials for their potential to treat obesity, there is still an urgent need for new drugs targeting the world-wide obesity problem.

One approach to the development of drugs for the treatment of obesity is to target the melanocortin system, which includes a family of five G-protein-coupled receptors, the melanocortin receptors (MCR),[3] named MCR1–5 in the order of their discovery (8–12). The endogenous peptide agonists, adrenocorticotropic hormone and α-, β-, and γ-melanocyte-stimulating hormone (MSH), all derived from the precursor protein pro-opiomelanocortin, form part of the system, in addition to the inverse agonists agouti protein and agouti-related protein.

The five MCRs are distributed throughout the body and are associated with a variety of physiological effects. MC1R is mainly present in melanocytes and melanoma cells (8, 9).

[3] The abbreviations used are: MCR, melanocortin receptor; CCK, cyclic cystine knot; MSH, melanocyte-stimulating hormone; Boc, *t*-butoxycarbonyl.

Novel Melanocortin Agonists Based on the Kalata B1 Scaffold

MC2R is present in the adrenal cortex, where it regulates steroidogenesis, and is only activated by adrenocorticotropic hormone, in contrast to the other MCRs (8). MC3R is mainly expressed in the arcuate nucleus (13) but is also present in the gut (10). MC4R is found throughout the brain (14) and in the spinal cord and dorsal root ganglions (15). Stimulation of MC4R reduces food intake and increases the metabolic rate in mice (16), which makes it an interesting target for the treatment of obesity. MC5R is distributed throughout the body with high levels found in skeletal muscle, brain, and exocrine glands and has a variety of functions (12, 17, 18).

The MSH peptides and adrenocorticotropic hormone share the tetrapeptide His-Phe-Arg-Trp pharmacophore, which is the shortest peptide active on the MCRs (19). Various modifications to these peptides have been made to explore the role of individual amino acids. Substitution of Met^4 with norleucine (Nle) and modifying the conformation of Phe^7 to D-Phe in α-MSH (see Table 1) yielded a stable subnanomolar agonist named NDP-α-MSH (20). Additionally, it has been shown that the His-D-Phe-Arg-Trp tetrapeptide alone has nanomolar activity on the MC4R (21). In another study, a truncated analogue of the inverse agonist agouti-related protein was turned into a full agonist by exchanging the binding sequence with His-D-Phe-Arg-Trp (22). These findings suggest that it might be possible to graft the His-Phe-Arg-Trp sequence and related modified sequences into stable peptide frameworks to develop novel MCR agonists. The motivation for the grafting is to place the bioactive tetrapeptide in a molecular context where is will be less susceptible to proteolysis and will have more favorable biopharmaceutical properties than the isolated peptide sequence.

The concept of developing MC4R agonists for the treatment of obesity has been around for more than a decade, and agonists have been shown to have efficacy in rodent models of obesity (23). However, despite strenuous efforts, no compounds have reached clinical trials for the treatment of obesity. The similarity between the various MCRs, which makes it challenging to make selective agonists, and the generally low half-lives of peptides *in vivo* (24) have probably contributed to this lack of success.

Recent discoveries of naturally occurring stable peptides offer the potential to overcome some of the limitations of peptides as drug leads. In the mid-1990s, several ultra-stable peptides that had both a cyclic backbone and three disulfide bonds forming a cystine knot were discovered (25–28). The most extensively studied of these is the 29-residue peptide kalata B1 found in the African plant *Oldenlandia affinis* (26), which originally attracted attention because of its reported uterotonic activity (29). More recently, it has been reported to have antimicrobial (30) and cancer cell cytotoxic activity (31) as well as a range of other activities (32). Its biological function in the plant is thought to be as a host defense pesticidal agent, because it reduces the growth of the larvae of the crop pest *Helicoverpa punctigera* (33). Following additional discovery efforts (34–38) since these early studies, the group of cyclic cystine-knotted (CCK) peptides now includes several hundred sequences and has been given the name cyclotides (35, 39). They are exceptionally stable toward enzymatic or thermal degradation because of their cyclic backbone and cystine knot (26, 28, 40).

Because of their stability and large sequence variation in nature, cyclotides have been suggested as promising scaffolds for the grafting of pharmaceutically interesting peptides to stabilize them (35, 41). There are six backbone loops decorating the cystine knot core, and these offer opportunities for conformational control of a variety of peptide epitopes. In addition to being amenable to solid phase peptide synthesis (30, 42), cyclotide libraries have recently been expressed in bacterial cells (43), thus providing alternative routes to their manufacture.

There are currently only a few examples demonstrating the grafting of biologically active sequences into cyclotides or related acyclic cystine knot scaffolds. For example, Clark *et al.* (44) demonstrated that it was possible to substitute selected amino acids in loop 5 of kalata B1 to remove intrinsic hemolytic activity but retain the native fold, and later studies on this framework demonstrated efficacy for grafted antiangiogenic sequences (45) and bradykinin antagonists (46). Thongyoo *et al.* (47) changed the specificity of the trypsin inhibitor cyclotide, MCoTI-II, toward other proteases with one to three amino acid substitutions, and Chan *et al.* (48) reported a novel angiogenic agent based on this framework. In acyclic cystine-knotted peptides, Reiss *et al.* (49) successfully grafted platelet aggregation inhibiting sequences, and as mentioned above, agouti-related protein was turned into a full agonist on the melanocortin receptors (22).

In this study, kalata B1 was used as a scaffold for the insertion (grafting) of melanocortin receptor-activating sequences. The grafted sequences are shown in Fig. 1 along with the NMR-derived structure of kalata B1. These analogues have the potential to become leads for a new class of melanocortin receptor agonists for the treatment of obesity. More broadly, they will expand knowledge on the applicability of cyclotides as scaffolds.

EXPERIMENTAL PROCEDURES

Peptide Synthesis—Peptides were synthesized manually by Boc solid phase peptide synthesis on a Boc-Gly-phenylacetamidomethyl resin using 2-(1-*H*-benzotriazol-1-yl)-1,1,3,3-tetramethyluronium hexafluorophosphate or 2-(6-chloro-1-*H*-benzotriazol-1-yl)-1,1,3,3-tetramethylaminium hexafluorophosphate as coupling reagents, as described previously (44). Mercaptopropionic acid was used as a linker to facilitate backbone cyclization by native chemical ligation (50). Peptides were cleaved from the resin using hydrogen fluoride/cresol/thiocresol (50:4:1 v/v/v), precipitated in diethyl ether, and lyophilized. The crude peptides were purified using HPLC with a gradient of 25–45% solvent B (90% acetonitrile, 0.1% TFA in water) against solvent A (0.1% TFA in water) over 40 min. A Phenomenex C$_{18}$ column was used and absorbance measured at 280 nm. Backbone cyclization and disulfide bonds were formed using 0.1 M ammonium bicarbonate (pH 8.2), isopropyl alcohol (50:50, v/v) buffer for 48 h, at a peptide concentration of 0.2 mg/ml. At 0 and 24 h, 1 mM reduced glutathione was added. The oxidized peptides were purified on HPLC with 30–50% solvent B over 60 min. The peptides were characterized using electrospray ionization mass spectrometry; the purity was determined by RP-ultra-performance liquid chromatography, and the peptides were quantified using a chemiluminescent nitrogen detector (51).

NMR—Peptides were dissolved at a concentration of ~1 mM in 10% D_2O and 90% H_2O. Spectra were recorded at 298 K on a Bruker AVANCE 600 MHz NMR spectrometer. Two-dimensional spectra recorded included TOCSY, NOESY, and DQF-COSY. The mixing times for the TOCSY and NOESY spectra were 80 and 200 ms, respectively. The processed spectra were analyzed using the program CcpNMR Analysis, University of Cambridge, UK. Three-dimensional structures were calculated from the recorded two-dimensional spectra using CYANA as described previously (52). Structures were analyzed using Molprobity and PROMOTIF (53) and displayed using MolMol (54) and PyMol (55). Structures and chemical shifts have been deposited in the Protein Data Bank (Protein Data Bank code 2lur) and Biomagnetic Resonance Bank (BMRB ID 18536), respectively.

Melanocortin Assays—Melanocortin receptor binding assays were conducted as described previously (56). Each assay was performed in duplicate, and three assays were done on each receptor. Peptides (3 pM to 3 μM) were incubated with homogenized membranes from baby hamster kidney cells expressing the various MCRs and ^{125}I-NDP-α-MSH (around 60,000 counts/min). The incubation was stopped after 1 h by filtration through polyethyleneimine-treated filter plates. Scintillation liquid was added to the plates, and the radioactivity was counted.

The cAMP activity assays were conducted on baby hamster kidney cells expressing the MC4R, using the FlashPlate™ assay as described previously (56). Cells and peptide (100 fM to 10 μM to) were incubated and shaken for 30 min at room temperature. Detection mixture was added according to FlashPlate protocol, shaken for 30 min, and incubated overnight. The amount of cAMP produced was measured by displacement of radiolabeled cAMP bound to anti-cAMP antibodies in accordance with the FlashPlate protocol.

The data analyses from the receptor assays were performed as described previously (56), using the program GraphPad Prism, GraphPad Software. IC_{50} values were calculated using a nonlinear regression model, and K_i values were calculated from the IC_{50} values. The potency at the MC4R was determined as EC_{50} values, calculated by nonlinear regression of the activity assay data.

Enzymatic Cleavage Assays—Peptides were incubated with chymotrypsin (1:5 w/w enzyme/peptide ratio) at 37 °C. For α-MSH, the ratio was 1:10 w/w enzyme/peptide to have close to equal molar ratios for all peptides. Samples were aliquoted out and quenched with TFA before analysis on ultra-performance liquid chromatography. Peak heights were used to calculate the amount of intact peptide.

RESULTS

Design, Synthesis, and Characterization of the Grafted Peptides—Four melanocortin analogues of kalata B1 were synthesized using solid phase Boc chemistry. The sequences of the peptides are shown in Table 1. They are named to reflect the grafted epitopes incorporated into the kalata B1 (kB1) sequence. For example, kB1(HFRW;24–27) indicates replacement of residues 24–27 in loop 6 of kalata B1 (kB1) with the HFRW (His-Phe-Arg-Trp) tetrapeptide sequence. In this case,

TABLE 1

Nomenclature, sequences, and disulfide pattern of grafted cyclotides with their corresponding masses

The sequence of α-MSH is shown below.

Peptide	Primary structure	Calculated mass (Da)[a]	Observed mass (Da)[a]
kalata B1	CGETCVGGTCNTPGCTCSWPVCTRNGLPV	2890.1	2890.0
kB1[GHFRWG;23-28]	CGETCVGGTCNTPGCTCSWPVCGHFRWGV	2992.1	2992.0
kB1[GHfRWG;23-28]	CGETCVGGTCNTPGCTCSWPVCGHfRWGV	2992.1	2991.9
kB1[HFRW;24-27]	CGETCVGGTCNTPGCTCSWPVCTHFRWPV	3076.2	3076.1
kB1[HfRW;24-27]	CGETCVGGTCNTPGCTCSWPVCTHfRWPV	3076.2	3076.1
	1 5 10 15 20 25		
α-MSH	Ac-SYSMEHFRWGKPV		

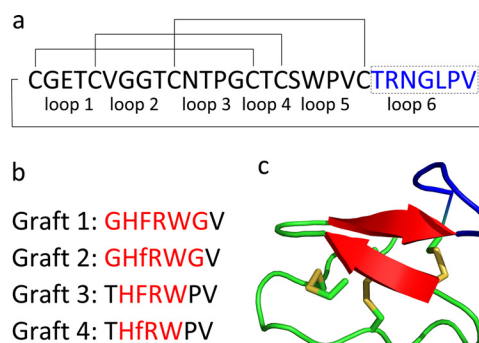[a] Monoisotopic mass is indicated.

FIGURE 1. *a,* primary sequence of kalata B1. The disulfide bonds and circular backbone are indicated with *lines,* and the inter-cysteine loops are labeled *below* the sequence. Loop 6, in which the melanocortin sequences are grafted, is highlighted in *blue. b,* four sequences grafted into loop 6. The lowercase *f* refers to D-Phe. Non-native kalata B1 residues are highlighted in *red. c,* structure of kalata B1 (Protein Data Bank code 1nb1), with disulfides indicated, and loop 6 highlighted in *blue* (62).

the tetrapeptide is flanked by the remaining native amino acids in loop 6, *i.e.* T at the N-terminal side and PV at the C-terminal side, making the total composition of loop 6 THFRWPV in place of the native TRNGLPV. To account for the possibility that direct replacements might constrain the bioactive tetrapeptide in a nonactive conformation, other grafts were made where flanking glycine residues were used in place of the native kalata B1 residues.

The peptides were assembled attached to a C-terminal mercaptopropionic acid linker to facilitate subsequent cyclization of the termini. The linear precursor peptides were synthesized with Val[21] as the C terminus, because this allowed the synthesis of one batch of resin to which was coupled the first 22 amino acids common to all analogues. This batch was subsequently split to continue separate synthesis of the differing parts of the four analogues. Loop 6 was chosen as the site for grafting the melanocortin sequence, because it is the largest of the inter-cysteine loops in kalata B1. In addition, the structure of kalata B1 shown in Fig. 1 indicates that the other loops are not in close proximity with loop 6 and therefore are not likely to interfere with the presentation of the grafted melanocortin sequence to the MCRs.

The peptides were cleaved from the resin and then oxidized and cyclized in a single step at 0.2 mg/ml concentration in a 0.1 M ammonium bicarbonate (pH 8.2), isopropyl alcohol (50:50, v/v) buffer for 48 h with 1 mM reduced glutathione added at 0
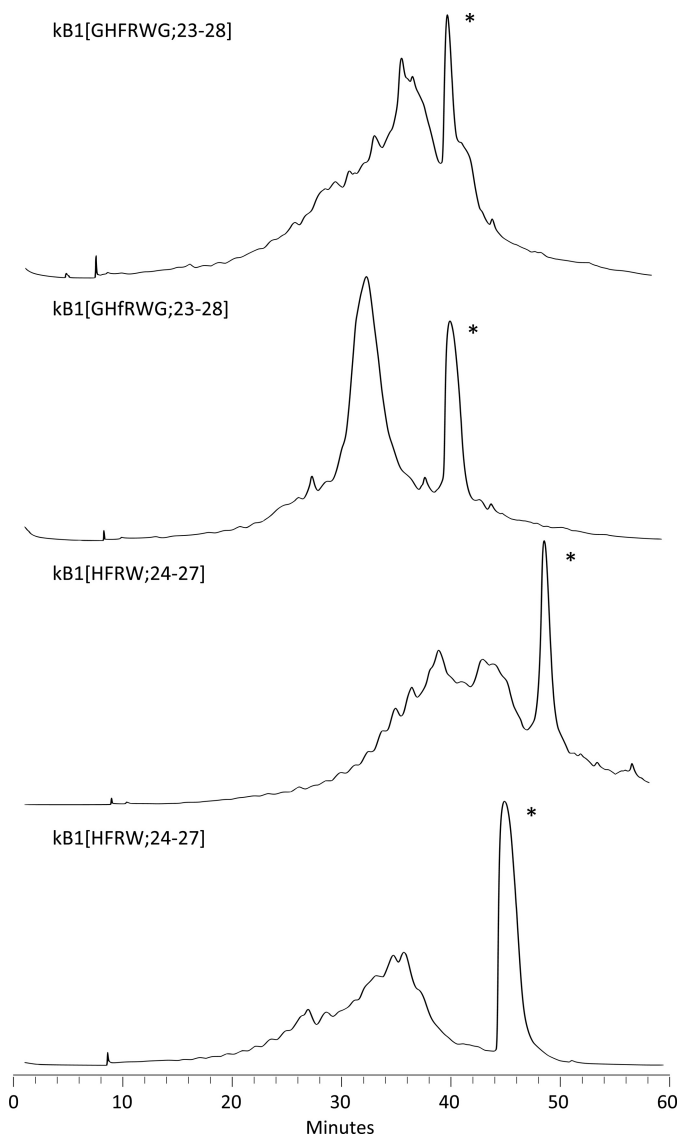
FIGURE 2. **Chromatograms from the preparative HPLC purifications of the grafted peptides.** The peaks corresponding to the correctly folded peptides are marked with an *asterisk*.

and 24 h. Chromatograms from the purification of the folded peptides are shown in Fig. 2.

The late eluting peaks were purified and analyzed by NMR spectroscopy to confirm that the native fold was present. A comparison of the Hα chemical shifts of the grafted peptides with the native peptide is shown in Fig. 3. The comparison indicates that the overall structures of the peptides are similar. The only Hα chemical shift differences larger than 0.2 ppm were found for Val[29], which is the C-terminal neighbor to the grafted sequence, Cys[1], which is bound to Val[29], and Cys[15], which forms a disulfide with Cys[1]. The peptides kB1(HFRW;24–27) and kB1(HfRW;24–27) had additional peaks in the NMR spectra (data not shown) deriving from *cis/trans*-isomerization at the Trp[27]/Pro[28] peptide bond. The major conformation, judging from the intensity of the peaks, was the *cis*-Pro conformation. The two conformers of kB1(HfRW;24–27) were distinguished by a strong NOE cross-peak between the Hα-Hα protons of Trp[27] and Pro[28] (4.24

ppm; 3.33 ppm) in the major conformation and a weaker NOE cross-peak between Hα-Hδ protons (5.01 ppm; 3.91 ppm) in the minor conformation.

Melanocortin Assays—The binding affinities of the four synthesized melanocortin analogues of kalata B1 to MCR1 and MCR3–5 were determined by competition binding assays using radiolabeled NDP-α-MSH. Kalata B1 and α-MSH were also evaluated as controls. The results are given in Table 2, and results from binding studies of kalata B1, kB1(GHFRWG;23–28) and α-MSH at the MC4R are shown in Fig. 4. Peptide kB1(GHFRWG;23–28) had a K_i of 29 nM at the MC4R and was 107 or 314 times selective for the MC4R over the MC1R or MC5R, respectively. The peptide did not bind to the MC3R. The K_i value of α-MSH at the MC4R receptor was 39 nM. Peptide kB1(GHFRWG;23–28) was also tested in a functional assay to evaluate the potency at the MC4R and was found to have an EC$_{50}$ of 580 nM, whereas α-MSH had an EC$_{50}$ of 3.7 nM (Table 2).

Three-dimensional Structure of kB1(GHFRWG;23–28)—Given the potency and selectivity observed for kB1(GHFRWG;23–28), its three-dimensional structure was determined to provide insight into structure-activity relationships. Structures were determined using torsion angle dynamics in the program CYANA, and the 20 structures with the lowest target function were chosen to represent the global fold. Energetic and geometric statistics are given in Table 3. Analysis of the structures with PROMOTIF (53) revealed that the major element of secondary structure is a β-hairpin involving residues 16–18 and 21–23. A third strand comprising residues 3–4 is associated with the hairpin to form a triple-stranded β-sheet as shown in Fig. 5. In addition, residues 5–8 form a type I β-turn, and residues 10–12 and 12–14 form inverse γ-turns. Comparison of the structure of kB1(GHFRWG;23–28) with the native kalata B1 framework indicates that the overall fold is maintained. The cyclic cystine knot motif and β-hairpin are the defining structural features of the cyclotides, and both are present in kB1(GHFRWG;23–28), despite the sequence changes in loop 6. The introduction of non-native sequences into the CCK scaffold can sometimes lead to disordered loops (45, 48). However, for kB1(GHFRWG; 23–28) the grafted loop 6 is as well defined as the other loops, with order parameters >0.93 for the ϕ and φ angles over the whole molecule.

The grafted sequence has several large hydrophobic residues, including His, Phe, and Trp as shown in Fig. 5b, and it was of interest to determine how their presence might influence the nature of the molecular surface. Analysis of the surface of kB1(GHFRWG;23–28) shows that a group of surface-exposed hydrophobic residues is punctated by polar or charged residues. In addition, the arginine in loop 6 is highly solvent-exposed. A similar distribution of surface residues is evident in kalata B1, with the exception of loop 6, as illustrated in Fig. 6.

Proteolytic Stability—To investigate the stability of the peptides, kalata B1, kB1(GHFRWG;23–28) and α-MSH were incubated with chymotrypsin. As shown in Fig. 7, more than 95% of kalata B1 remained intact for 5 h. Peptide kB1(GHFRWG;23–28) was slightly less stable, but around 80% was intact after 5 h. After 24 h, the amounts of intact peptide had not changed further, but this is probably due to auto-cleavage and deactivation of chymotrypsin by this time. Compared with kalata B1,
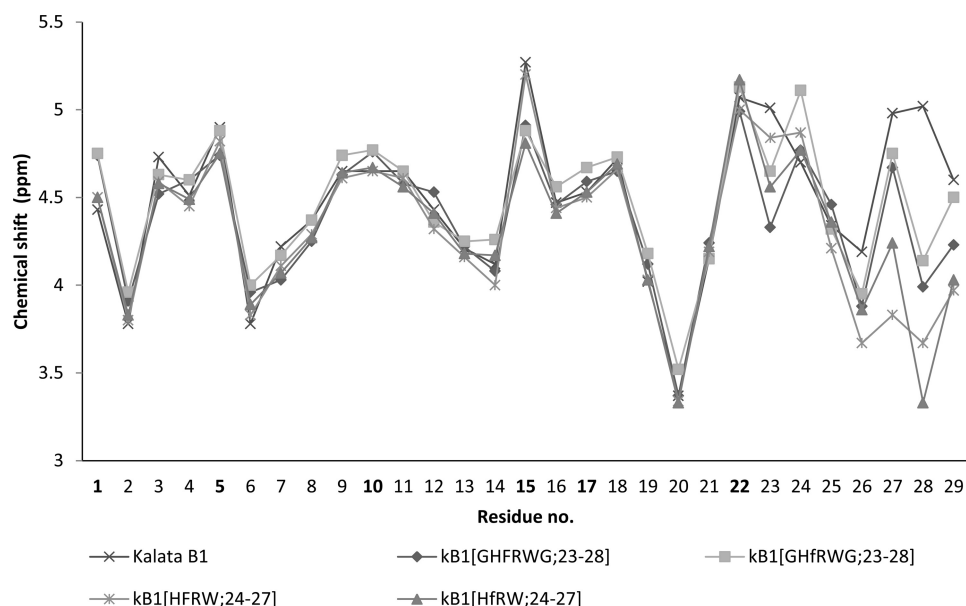
FIGURE 3. Hα chemical shifts of the four synthesized peptides and kalata B1. The *numbers* corresponding to cysteine residues are highlighted in *boldface*.

TABLE 2

Binding affinity of grafted cyclotides for melanocortin receptors 1 and 3–5 and functional activity at MCR4 of the most potent binder

NA means no activity (*i.e.* K_i >10,000 nM). Data represent an average pK_i of three replicates $\pm$ S.E. K_i value (in parentheses) is calculated from the average pK_i value. Potency at the MC4R was determined only for kB1(GHFRWG;23–28).

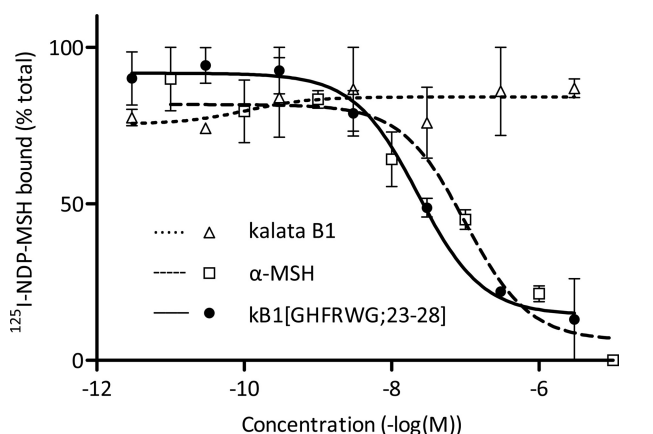| Peptide	hMC1R, pK_i	hMC3R, pK_i	hMC4R, pK_i	hMC4R, cAMP pEC$_{50}$	hMC5R, pK_i
	K_i/nM	K_i/nM	K_i/nM	EC_{50}/nM	K_i/nM
Kalata B1	NA	NA	NA		NA
kB1(GHFRWG;23–28)	5.50 $\pm$ 0.09 (3,100)	NA	7.53 $\pm$ 0.28 (29)	6.24 $\pm$ 0.08 (580)	5.04 $\pm$ 0.14 (9,100)
kB1(GHfRWG;23–28)	6.37 $\pm$ 0.06 (420)	5.11 $\pm$ 0.03 (7,700)	6.59 $\pm$ 0.15 (250)		5.30 $\pm$ 0.04 (5,000)
kB1(HFRW;24–27)	NA	NA	NA		NA
kB1(HfRW;24–27)	NA	Na	NA		NA
α-MSH	9.16 $\pm$ 0.05 (0.69)	7.51 $\pm$ 0.04 (31)	7.41 $\pm$ 0.26 (39)	8.44 $\pm$ 0.26 (3.7)	6.75 $\pm$ 0.16 (180)

FIGURE 4. MC4R binding assays for kB1(GHFRWG;23–28), kalata B1 and α-MSH. Each assay was performed in duplicate. Cell membranes expressing the MC4R were incubated with ^{125}I-NDP-α-MSH and the synthesized peptides. The amount of radioactivity from bound ^{125}I-NDP-α-MSH was counted, and K_i values were calculated. Data points are average values from the assays, and S.E. values are indicated with *error bars*.

TABLE 3

NMR and refinement statistics for the structure of kB1(GHFRWG;23–28)

NMR distance and dihedral constraints	
Distance constraints	
Total NOE	291
Short range ($|i − j|$<1)	202
Medium range (1$\langle$($|i − j|$<5)	42
Long range ($|i − j|\geq$5)	47
Dihedral angle constraints	
ϕ	12
Structure statistics	
CYANA target function	1.02 $\pm$ 0.07
Violations (mean $\pm$ S.D.)	
Distance constraints, r.m.s.d.	0.01 $\pm$ 0.002 Å
Dihedral angle constraints, r.m.s.d.	1.45 $\pm$ 0.12°
Maximum distance constraint violation	0.26 Å
Max. dihedral angle violation	1.01°
Average pairwise r.m.s.d.[a]	
Backbone	0.41 $\pm$ 0.11 Å
Heavy	0.84 $\pm$ 0.18 Å
Ramachandran statistics	
Residues is most favored regions	49.5%
Residues in additionally allowed regions	50.5%

[a] Pairwise root mean square deviation (r.m.s.d.) was calculated from the 20 structures with the lowest target function.

kB1(GHFRWG;23–28) has two additional potential chymotrypsin cleavage sites in the grafted sequence, so the observed resistance to proteolysis is a significant finding. Finally, α-MSH completely degraded within 10 min.

DISCUSSION

In this study we used the kalata B1 cyclotide scaffold to design a novel agonist for the MC4R. This analogue (kB1(GHFRWG;23–28)) also showed selectivity over other
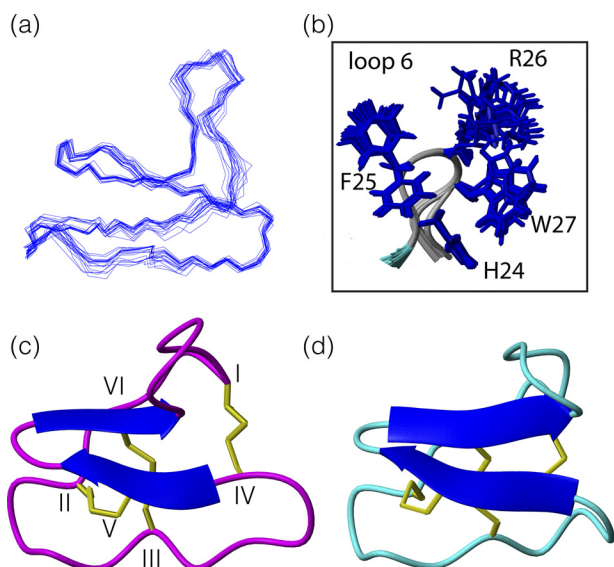
FIGURE 5. *a,* overlay of the 20 minimum energy structures of kB1(GHFRWG; 23–28). *b,* overlay highlighting the side chains of loop 6 shown in *stick* format. *c, ribbon* model of the NMR-derived structure of kB1(GHFRWG;23–28). Protein Data Bank code 2lur. *d, ribbon* model of kalata B1. Protein Data Bank code 1nb1.
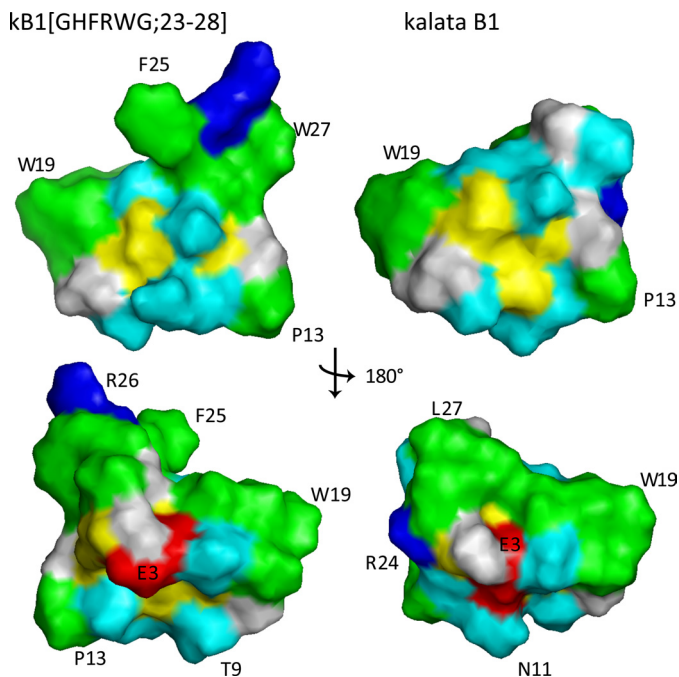

FIGURE 6. **Surface representation of kB1(GHFRWG;23–28) (*left*) and kalata B1 (*right*).** The only major differences are observed in the grafted loop 6, *i.e.* residues 23–28. Hydrophobic residues are highlighted in *green*, positively charged in *blue*, negatively charged in *red*, cysteines in *yellow,* and polar in *cyan*. The *top views* have similar orientation as the *ribbon* models in Fig. 5. The residues *F25*, *R26*, and *W27* in kB1(GHFRWG;23–28) are part of the melanocortin pharmacophore grafted into loop 6 of kalata B1.

MCRs tested, highlighting the potential of the CCK scaffold for targeting specific interactions implicated in the regulation of appetite and energy homeostasis and providing a possible lead molecule for the treatment of obesity. Interestingly, kB1(GHFRWG;23–28) showed higher affinity for the MC4R compared with the native agonist α-MSH, but it was not as potent functionally. It appears likely that kB1(GHFRWG;23–

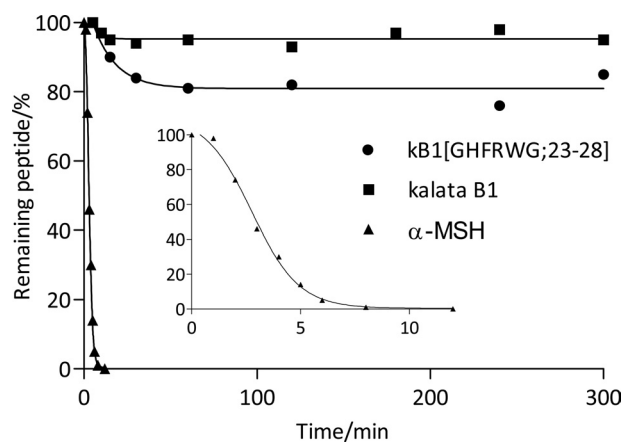FIGURE 7. **Enzymatic stability of kalata B1, kB1(GHFRWG;23–28), and α-MSH toward chymotrypsin cleavage.** The peptides were incubated with chymotrypsin for 5 h at 37 °C. The enzyme to peptide ratio was 1:5 w/w (1:10 w/w for α-MSH to have equal molar ratios). The *inset* shows the degradation of α-MSH the first 10 min of incubation.

28) has stronger binding to the active site than α-MSH, but due to the placement of the pharmacophore within the kalata B1 scaffold and possible steric clashes with the receptor, it is not able to induce a similar conformational change in the receptor, which is required for full activation of the cAMP cascade. Nevertheless, significant (sub-micromolar) activation of the cAMP response was observed. This successful example of grafting a function into a cyclotide adds to a growing body of evidence that the CCK framework can accommodate a diverse range of bioactivities.

Four analogues of kalata B1 were synthesized using Boc chemistry and generally folded well using the oxidation conditions previously established for native kalata B1 (Fig. 2). All of the analogues retained the native fold based on analysis with NMR spectroscopy. Even though six of the seven residues in loop 6 were replaced, the CCK holds the remaining loops in place and allows these changes in loop 6. The grafted sequence is significantly more hydrophobic than sequences previously grafted into this framework, and this study expands the known sequence diversity accommodated by the cyclotide scaffold (44–46, 48), and in particular highlights the tolerance of loop 6 to changes. This tolerance is further demonstrated by observations that loop 6 can be truncated and opened to produce acyclic cystine knot derivatives that maintain the same global fold as kalata B1 (57). In essence, the exposed loops of the CCK framework can be regarded as "plug and play" cassettes that can be substituted to introduce a desired biological activity.

Interestingly, kB1(GHfRWG;23–28), the D-Phe[25] analogue of kB1(GHFRWG;23–28) bound with lower affinity to the MCRs than the all-L graft. This was surprising because D-Phe analogues of short linear peptides are known to have higher affinity for the MCRs compared with the L-Phe analogues (20). The locked conformation of the pharmacophore in loop 6 of kalata B1 could change the presentation to the active site of the receptors and consequently be an explanation for this observation. There is clearly potential for further optimization of the bioactive epitope, and these studies are planned in our laboratory.

NMR spectra for kB1(HFRW;24–27) and kB1(HfRW;24–27) revealed that two conformations were present. This conformational heterogeneity appears to be related to *cis/trans*-isomerization around Pro[28]. The major conformation, based on inter-residue cross-peaks was the *cis*-conformation. This was confirmed by a strong Hα-Hα cross-peak between Trp[27] and Pro[28]. The *cis*-Pro conformation is consistent with what has previously been described for the Trp[19]–Pro[20] bond in kalata B1 (35, 58). The strong Hα-Hα cross-peak between Trp[19] and Pro[20] was observed in all peptides, whereas a Hα-Hδ cross-peak was observed for the Thr[12]–Pro[13] bond. The *cis*-Pro[20] bond causes a conceptual twist in the backbone, which defines the Möbius family of cyclotides (35). The additional twist caused by the *cis*-Pro[28] bond changes the topology of kB1(HFRW;24–27) and kB1(HfRW;24–27). This could be part of the reason why they did not bind to the MCRs, because a twist in the backbone around the pharmacophore changes the presentation of the side chains at the active site of the receptors. Besides the conformational change, it is also possible that the side chains of Thr[23] and Pro[28] in kB1(HFRW;24–27) and kB1(HfRW;24–27) affect the binding of the pharmacophore to the active site of the MCRs negatively compared with Gly[23] and Gly[28] in kB1(GHFRWG;23–28) and kB1(GHfRWG;23–28), which due to their lack of side chain would interfere less with the active site.

The intrinsic resistance of α-MSH to proteolytic degradation is very low but can be somewhat increased by engineering a single disulfide in the sequence (59). Kalata B1 has been demonstrated to have significantly increased stability toward enzymatic degradation compared with noncystine-knotted analogues, linear cystine-knotted peptides, and noncyclic peptides (40). It was of interest to determine whether the target-grafting epitope would have enhanced resistance to proteolysis when incorporated into the cyclotide framework. Chymotrypsin cleavage assays for kB1(GHFRWG;23–28), kalata B1, and α-MSH confirmed this expectation. Whereas α-MSH was completely degraded within 10 min under the conditions studied, kalata B1 was 95% intact after 5 h and remained stable even after 24 h, probably due to auto-cleavage of chymotrypsin. KB1(GHFRWG;23–28) was only slightly less stable than kalata B1, being 80% intact after 5 h. This marginal loss of stability is surprising on the one hand because the grafted sequence in loop 6 contains two potential chymotrypsin cleavage sites and hence the sequence is intrinsically susceptible to proteolysis. On the other hand, the results provide clear confirmation of the ability of the cyclotide framework to stabilize even a "susceptible" epitope. The observation that kB1(GHFRWG;23–28) was more than 80% intact after extended incubation with chymotrypsin confirms the high stability toward enzymatic degradation of both kalata B1 and grafted analogues thereof.

Cyclotides and other cystine knot micro-proteins have been suggested to have the potential for oral delivery, partly because of their high stability (60, 61). This potential was recently demonstrated in the development of an analogue of kalata B1 that is orally active in a mouse model of inflammatory pain (46), suggesting that similar exciting results for the oral route of drug delivery might be achieved with other examples of kalata B1

grafting. The analogues of kalata B1 reported here represent a new group of selective melanocortin agonists. Because of their cyclotide framework, they are more stable than previously reported linear and mono-cyclic melanocortin analogues, and with further optimization this group of peptides could provide new peptide-based leads with the potential to treat obesity.

REFERENCES

1. Finucane, M. M., Stevens, G. A., Cowan, M. J., Danaei, G., Lin, J. K., Paciorek, C. J., Singh, G. M., Gutierrez, H. R., Lu, Y., Bahalim, A. N., Farzadfar, F., Riley, L. M., and Ezzati, M. (2011) National, regional, and global trends in body-mass index since 1980. Systematic analysis of health examination surveys and epidemiological studies with 960 country-years and 9.1 million participants. *Lancet* **377,** 557–567
2. Stevens, J., Couper, D., Pankow, J., Folsom, A. R., Duncan, B. B., Nieto, F. J., Jones, D., and Tyroler, H. A. (2001) Sensitivity and specificity of anthropometrics for the prediction of diabetes in a biracial cohort. *Obes. Res.* **9,** 696–705
3. Wannamethee, S. G., Shaper, A. G., Durrington, P. N., and Perry, I. J. (1998) Hypertension, serum insulin, obesity, and the metabolic syndrome. *J. Hum. Hypertens.* **12,** 735–741
4. Wolf, H. K., Tuomilehto, J., Kuulasmaa, K., Domarkiene, S., Cepaitis, Z., Molarius, A., Sans, S., Dobson, A., Keil, U., and Rywik, S. (1997) Blood pressure levels in the 41 populations of the WHO MONICA Project. *J. Hum. Hypertens.* **11,** 733–742
5. Miller, W. C., Koceja, D. M., and Hamilton, E. J. (1997) A meta-analysis of the past 25 years of weight loss research using diet, exercise, or diet plus exercise intervention. *Int. J. Obes. Relat. Metab. Disord.* **21,** 941–947
6. Expert Panel on Detection, Evaluation, and Treatment of High Blood Cholesterol in Adults (2001) Executive Summary of The Third Report of The National Cholesterol Education Program (NCEP) Expert Panel on Detection, Evaluation, and Treatment of High Blood Cholesterol in Adults (Adult Treatment Panel III). *JAMA* **285,** 2486–2497
7. Wright, S. M., and Aronne, L. J. (2011) Obesity in 2010. The future of obesity medicine. Where do we go from here? *Nat. Rev. Endocrinol.* **7,** 69–70
8. Mountjoy, K. G., Robbins, L. S., Mortrud, M. T., and Cone, R. D. (1992) The cloning of a family of genes that encode the melanocortin receptors. *Science* **257,** 1248–1251
9. Chhajlani, V., and Wikberg, J. E. (1992) Molecular cloning and expression of the human melanocyte-stimulating hormone receptor cDNA. *FEBS Lett.* **309,** 417–420
10. Gantz, I., Konda, Y., Tashiro, T., Shimoto, Y., Miwa, H., Munzert, G., Watson, S. J., DelValle, J., and Yamada, T. (1993) Molecular cloning of a novel melanocortin receptor. *J. Biol. Chem.* **268,** 8246–8250
11. Gantz, I., Miwa, H., Konda, Y., Shimoto, Y., Tashiro, T., Watson, S. J., DelValle, J., and Yamada, T. (1993) Molecular cloning, expression, and gene localization of a fourth melanocortin receptor. *J. Biol. Chem.* **268,** 15174–15179
12. Chhajlani, V., Muceniece, R., and Wikberg, J. E. (1993) Molecular cloning of a novel human melanocortin receptor. *Biochem. Biophys. Res. Commun.* **195,** 866–873
13. Roselli-Rehfuss, L., Mountjoy, K. G., Robbins, L. S., Mortrud, M. T., Low, M. J., Tatro, J. B., Entwistle, M. L., Simerly, R. B., and Cone, R. D. (1993) Identification of a receptor for γ-melanotropin and other proopiomelanocortin peptides in the hypothalamus and limbic system. *Proc. Natl. Acad. Sci. U.S.A.* **90,** 8856–8860
14. Mountjoy, K. G., Mortrud, M. T., Low, M. J., Simerly, R. B., and Cone, R. D. (1994) Localization of the melanocortin-4 receptor (MC4-R) in neuroendocrine and autonomic control circuits in the brain. *Mol. Endocrinol.* **8,** 1298–1308
15. Starowicz, K., Bilecki, W., Sieja, A., Przewlocka, B., and Przewlocki, R. (2004) Melanocortin 4 receptor is expressed in the dorsal root ganglions and down-regulated in neuropathic rats. *Neurosci. Lett.* **358,** 79–82
16. Chen, A. S., Metzger, J. M., Trumbauer, M. E., Guan, X. M., Yu, H., Frazier, E. G., Marsh, D. J., Forrest, M. J., Gopal-Truter, S., Fisher, J., Camacho, R. E., Strack, A. M., Mellin, T. N., MacIntyre, D. E., Chen, H. Y., and Van

der Ploeg, L. H. (2000) Role of the melanocortin-4 receptor in metabolic rate and food intake in mice. *Transgenic Res.* **9,** 145–154

17. Chen, W., Kelly, M. A., Opitz-Araya, X., Thomas, R. E., Low, M. J., and Cone, R. D. (1997) Exocrine gland dysfunction in MC5-R-deficient mice. Evidence for coordinated regulation of exocrine gland function by melanocortin peptides. *Cell* **91,** 789–798

18. Fathi, Z., Iben, L. G., and Parker, E. M. (1995) Cloning, expression, and tissue distribution of a fifth melanocortin receptor subtype. *Neurochem. Res.* **20,** 107–113

19. Hruby, V. J., Wilkes, B. C., Hadley, M. E., Al-Obeidi, F., Sawyer, T. K., Staples, D. J., de Vaux, A. E., Dym, O., Castrucci, A. M., and Hintz, M. F. (1987) α-Melanotropin. The minimal active sequence in the frog skin bioassay. *J. Med. Chem.* **30,** 2126–2130

20. Sawyer, T. K., Sanfilippo, P. J., Hruby, V. J., Engel, M. H., Heward, C. B., Burnett, J. B., and Hadley, M. E. (1980) 4-Norleucine, 7-D-phenylalanine-α-melanocyte-stimulating hormone. A highly potent α-melanotropin with ultralong biological activity. *Proc. Natl. Acad. Sci. U.S.A.* **77,** 5754–5758

21. Haskell-Luevano, C., Holder, J. R., Monck, E. K., and Bauzo, R. M. (2001) Characterization of melanocortin NDP-MSH agonist peptide fragments at the mouse central and peripheral melanocortin receptors. *J. Med. Chem.* **44,** 2247–2252

22. Wilczynski, A., Wang, X. S., Joseph, C. G., Xiang, Z., Bauzo, R. M., Scott, J. W., Sorensen, N. B., Shaw, A. M., Millard, W. J., Richards, N. G., and Haskell-Luevano, C. (2004) Identification of putative agouti-related protein(87–132)-melanocortin-4 receptor interactions by homology molecular modeling and validation using chimeric peptide ligands. *J. Med. Chem.* **47,** 2194–2207

23. He, S., Ye, Z., Dobbelaar, P. H., Bakshi, R. K., Hong, Q., Dellureficio, J. P., Sebhat, I. K., Guo, L., Liu, J., Jian, T., Lai, Y., Franklin, C. L., Reibarkh, M., Holmes, M. A., Weinberg, D. H., MacNeil, T., Tang, R., Tamvakopoulos, C., Peng, Q., Miller, R. R., Stearns, R. A., Chen, H. Y., Chen, A. S., Strack, A. M., Fong, T. M., Wyvratt, M. J., Jr., and Nargund, R. P. (2010) Discovery of highly potent and efficacious MC4R agonists with spiroindane *N*-Me-1,2,4-triazole privileged structures for the treatment of obesity. *Bioorg. Med. Chem. Lett.* **20,** 6524–6565

24. Emmerson, P. J., Fisher, M. J., Yan, L. Z., and Mayer, J. P. (2007) Melanocortin-4 receptor agonists for the treatment of obesity. *Curr. Top. Med. Chem.* **7,** 1121–1130

25. Gustafson, K. R., Sowder, R. C., Henderson, L. E., Parsons, I. C., Kashman, Y., Cardellina, J. H., McMahon, J. B., Buckheit, R. W., Pannell, L. K., and Boyd, M. R. (1994) Circulins A and B. Novel human immunodeficiency virus (HIV)-inhibitory macrocyclic peptides from the tropical tree *Chassalia parvifolia*. *J. Am. Chem. Soc.* **116,** 9337–9338

26. Saether, O., Craik, D. J., Campbell, I. D., Sletten, K., Juul, J., and Norman, D. G. (1995) Elucidation of the primary and three-dimensional structure of the uterotonic polypeptide kalata B1. *Biochemistry* **34,** 4147–4158

27. Schöpke, T., Hasan Agha, M. I., Kraft, R., Otto, A., and Hiller, K. (1993) Hämolytisch aktive komponenten aus *Viola tricolor* L. und *Viola arvenses* Murray. *Sci. Pharm.* **61,** 145–153

28. Witherup, K. M., Bogusky, M. J., Anderson, P. S., Ramjit, H., Ransom, R. W., Wood, T., and Sardana, M. (1994) Cyclopsychotride A, a biologically active, 31-residue cyclic peptide isolated from *Psychotria longipes*. *J. Nat. Prod.* **57,** 1619–1625

29. Gran, L. (1973) Oxytocic principles of *Oldenlandia affinis*. *Lloydia* **36,** 174–178

30. Tam, J. P., Lu, Y. A., Yang, J. L., and Chiu, K. W. (1999) An unusual structural motif of antimicrobial peptides containing end-to-end macrocycle and cystine-knot disulfides. *Proc. Natl. Acad. Sci. U.S.A.* **96,** 8913–8918

31. Lindholm, P., Göransson, U., Johansson, S., Claeson, P., Gullbo, J., Larsson, R., Bohlin, L., and Backlund, A. (2002) Cyclotides. A novel type of cytotoxic agents. *Mol. Cancer Ther.* **1,** 365–369

32. Craik, D. J., Mylne, J. S., and Daly, N. L. (2010) Cyclotides. Macrocyclic peptides with applications in drug design and agriculture. *Cell. Mol. Life Sci.* **67,** 9–16

33. Jennings, C., West, J., Waine, C., Craik, D., and Anderson, M. (2001) Biosynthesis and insecticidal properties of plant cyclotides. The cyclic knotted proteins from *Oldenlandia affinis*. *Proc. Natl. Acad. Sci. U.S.A.* **98,** 10614–10619

34. Claeson, P., Göransson, U., Johansson, S., Luijendijk, T., and Bohlin, L. (1998) Fractionation protocol for the isolation of polypeptides from plant biomass. *J. Nat. Prod.* **61,** 77–81

35. Craik, D. J., Daly, N. L., Bond, T., and Waine, C. (1999) Plant cyclotides. A unique family of cyclic and knotted proteins that defines the cyclic cystine knot structural motif. *J. Mol. Biol.* **294,** 1327–1336

36. Göransson, U., Luijendijk, T., Johansson, S., Bohlin, L., and Claeson, P. (1999) Seven novel macrocyclic polypeptides from *Viola arvensis*. *J. Nat. Prod.* **62,** 283–286

37. Gruber, C. W., Elliott, A. G., Ireland, D. C., Delprete, P. G., Dessein, S., Göransson, U., Trabi, M., Wang, C. K., Kinghorn, A. B., Robbrecht, E., and Craik, D. J. (2008) Distribution and evolution of circular miniproteins in flowering plants. *Plant Cell* **20,** 2471–2483

38. Hernandez, J. F., Gagnon, J., Chiche, L., Nguyen, T. M., Andrieu, J. P., Heitz, A., Trinh Hong, T., Pham, T. T., and Le Nguyen, D. (2000) Squash trypsin inhibitors from *Momordica cochinchinensis* exhibit an atypical macrocyclic structure. *Biochemistry* **39,** 5722–5730

39. Wang, C. K., Kaas, Q., Chiche, L., and Craik, D. J. (2008) CyBase. A database of cyclic protein sequences and structures, with applications in protein discovery and engineering. *Nucleic Acids Res.* **36,** D206–D210

40. Colgrave, M. L., and Craik, D. J. (2004) Thermal, chemical, and enzymatic stability of the cyclotide kalata B1. The importance of the cyclic cystine knot. *Biochemistry* **43,** 5965–5975

41. Craik, D. J., Daly, N. L., and Waine, C. (2001) The cystine knot motif in toxins and implications for drug design. *Toxicon* **39,** 43–60

42. Daly, N. L., Love, S., Alewood, P. F., and Craik, D. J. (1999) Chemical synthesis and folding pathways of large cyclic polypeptides. Studies of the cystine knot polypeptide kalata B1. *Biochemistry* **38,** 10606–10614

43. Jagadish, K., and Camarero, J. A. (2010) Cyclotides, a promising molecular scaffold for peptide-based therapeutics. *Biopolymers* **94,** 611–616

44. Clark, R. J., Daly, N. L., and Craik, D. J. (2006) Structural plasticity of the cyclic cystine-knot framework. Implications for biological activity and drug design. *Biochem. J.* **394,** 85–93

45. Gunasekera, S., Foley, F. M., Clark, R. J., Sando, L., Fabri, L. J., Craik, D. J., and Daly, N. L. (2008) Engineering stabilized vascular endothelial growth factor-A antagonists: synthesis, structural characterization, and bioactivity of grafted analogues of cyclotides. *J. Med. Chem.* **51,** 7697–7704

46. Wong, C. T., Rowlands, D. K., Wong, C. H., Lo, T. W., Nguyen, G. K., Li, H. Y., and Tam, J. P. (2012) Orally active peptidic bradykinin B$_1$ receptor antagonists engineered from a cyclotide scaffold for inflammatory pain treatment. *Angew. Chem. Int. Ed. Engl.* **51,** 5620–5624

47. Thongyoo, P., Roqué-Rosell, N., Leatherbarrow, R. J., and Tate, E. W. (2008) Chemical and biomimetic total syntheses of natural and engineered MCoTI cyclotides. *Org. Biomol. Chem.* **6,** 1462–1470

48. Chan, L. Y., Gunasekera, S., Henriques, S. T., Worth, N. F., Le, S. J., Clark, R. J., Campbell, J. H., Craik, D. J., and Daly, N. L. (2011) Engineering pro-angiogenic peptides using stable, disulfide-rich cyclic scaffolds. *Blood* **118,** 6709–6717

49. Reiss, S., Sieber, M., Oberle, V., Wentzel, A., Spangenberg, P., Claus, R., Kolmar, H., and Lösche, W. (2006) Inhibition of platelet aggregation by grafting RGD and KGD sequences on the structural scaffold of small disulfide-rich proteins. *Platelets* **17,** 153–157

50. Dawson, P. E., Muir, T. W., Clark-Lewis, I., and Kent, S. B. (1994) Synthesis of proteins by native chemical ligation. *Science* **266,** 776–779

51. Fujinari, E. M., and Courthaudon, L. O. (1992) Nitrogen-specific liquid chromatography detector based on chemiluminescence. Application to the analysis of ammonium nitrogen in waste water. *J. Chromatogr. A* **592,** 209–214

52. Millard, E. L., Nevin, S. T., Loughnan, M. L., Nicke, A., Clark, R. J., Alewood, P. F., Lewis, R. J., Adams, D. J., Craik, D. J., and Daly, N. L. (2009) Inhibition of neuronal nicotinic acetylcholine receptor subtypes by α-conotoxin GID and analogues. *J. Biol. Chem.* **284,** 4944–4951

53. Hutchinson, E. G., and Thornton, J. M. (1996) PROMOTIF. A program to identify and analyze structural motifs in proteins. *Protein Sci.* **5,** 212–220

54. Koradi, R., Billeter, M., and Wüthrich, K. (1996) MOLMOL. A program for display and analysis of macromolecular structures. *J. Mol. Graph.* **14,** 29–32

ASBMB

55. DeLano, W. (2002) *The PyMOL Molecular Graphics System.* DeLano Scientific, San Carlos, CA

56. Conde-Frieboes, K., Thøgersen, H., Lau, J. F., Sensfuss, U., Hansen, T. K., Christensen, L., Spetzler, J., Olsen, H. B., Nilsson, C., Raun, K., Dahl, K., Hansen, B. S., and Wulff, B. S. (2012) Identification and *in vivo* and *in vitro* characterization of long acting and melanocortin 4 receptor (MC4-R)-selective α-melanocyte-stimulating hormone (α-MSH) analogues. *J. Med. Chem.* **55,** 1969–1977

57. Barry, D. G., Daly, N. L., Clark, R. J., Sando, L., and Craik, D. J. (2003) Linearization of a naturally occurring circular protein maintains structure but eliminates hemolytic activity. *Biochemistry* **42,** 6688–6695

58. Skjeldal, L., Gran, L., Sletten, K., and Volkman, B. F. (2002) Refined structure and metal-binding site of the kalata B1 peptide. *Arch. Biochem. Biophys.* **399,** 142–148

59. Castrucci, A. M., Hadley, M. E., Sawyer, T. K., and Hruby, V. J. (1984) Enzymological studies of melanotropins. *Comp. Biochem. Physiol. B* **78,** 519–524

60. Werle, M., Schmitz, T., Huang, H. L., Wentzel, A., Kolmar, H., and Bernkop-Schnürch, A. (2006) The potential of cystine-knot microproteins as novel pharmacophoric scaffolds in oral peptide drug delivery. *J. Drug Target.* **14,** 137–146

61. Daly, N. L., Rosengren, K. J., and Craik, D. J. (2009) Discovery, structure, and biological activities of cyclotides. *Adv. Drug Deliv. Rev.* **61,** 918–930

62. Rosengren, K. J., Daly, N. L., Plan, M. R., Waine, C., and Craik, D. J. (2003) Twists, knots, and rings in proteins. Structural definition of the cyclotide framework. *J. Biol. Chem.* **278,** 8606–8616